Contents

1. Tasks

The things that have to be done can be separated into two main exercises: the measurement of the spectrum of the absorption in iodine 2 and that of its emission. The precise tasks will now be listed.

1.1. Absorption

- The spectrum of the absorption of iodine molecules shall be measured.
- The vibration band of the progression $\nu'' = 0$ shall be identified.
- The vibration constants ω' and $\omega'_e x'_e$ are to be calculated with the Birge-Sponer-plot.
- The dissociation energy D_e shall be calculated with the Morse-potential and with the difference of terms.
- The stimulation energy T'_e and the energy at which the iodine molecule dissociates E_{diss} shall be calculated.
- The Morse-potential is to be drawn for the excited state.

1.2. Emission

- The spectrum of a mercury vapour lamp shall me measured in a range of 4000-6000 Å in order to calibrate the monochromator.
- The emission spectrum of the iodine molecule shall be drawn in a range from 6000 Å to 8000 Å.
- The monochromator shall be calibrated.
- The transmission, which has been initiated by the laser shall be identified.
- At last for five lines the Franck-Condon-factors are to be calculated and compared to the measured data.

2. Theoretical basics

The formulas and pictures of this chapter are, as long as not quoted otherwise, from [3].

2.1. Born-Oppenheimer-approximation

The main assumption of the Born-Oppenheimer approximation is, that the core of an atom moves much slower, than the electrons surrounding it. From this follows, that the configuration of the electrons follows the movement of the atom adiabatically and instantaneously [1]. This allows to separate the wave function of the electron and the core. This is described by the following formula from [7]

$$\Psi_k(\{r_i\},\{R_j\}) = \chi_k(\{R_j\}) \cdot \Psi_k^0(\{r_i\},\{R_j\}), \tag{2.1}$$

where the wave function of the core is given as $\chi_k(\{R_j\})$ and that of the electron as $\Psi_k^0(\{r_i\},\{R_j\})$. R_j gives the coordinates of the core and r_j that of the electron. The core wave function can be reduced further, by neglecting the rotation of the nucleon and just looking at the electronic and vibration transitions. This assumption is valid, because the energy differences from the rotation are around two magnitudes smaller than those resulting from the vibration.

2.2. Electronic transitions

The transition we are interested in this experiment is

$$\mathrm{X}^1\Sigma_{0g}^+ \leftrightarrow \mathrm{B}^3\Pi_{0u}^+. \tag{2.2}$$

It follows the selection rules for molecules and is the only possible transition:

- g $\leftrightarrow$ u, g $\nleftrightarrow$ g, u $\nleftrightarrow$ u
- $\Delta\Omega = 0, \pm 1$
- $\Delta\Lambda = 0, \pm 1$
- $\Delta\mathrm{S} = 0$

Ω is here the projection of the total angular momentum and Λ that of the orbital angular momentum on the axis of the molecule. S is the total spin of the electron. Because the last two selection rules don't always have to be true, it is no problem, that the last one gets violated by our transition. The coupling that follows from this violation of the last rule is called coupling case c. In such an electronic transition smaller transitions can be identified: vibration and rotation transitions. The relative intensities of the vibration levels are given by the so called Franck-Condon-factors, which we will discuss in subsection 2.3.

2.3. Franck-Condon-principle

The Franck-Condon-principle describes the probability of a transition between two energy levels in the sketch shown in Figure 1.

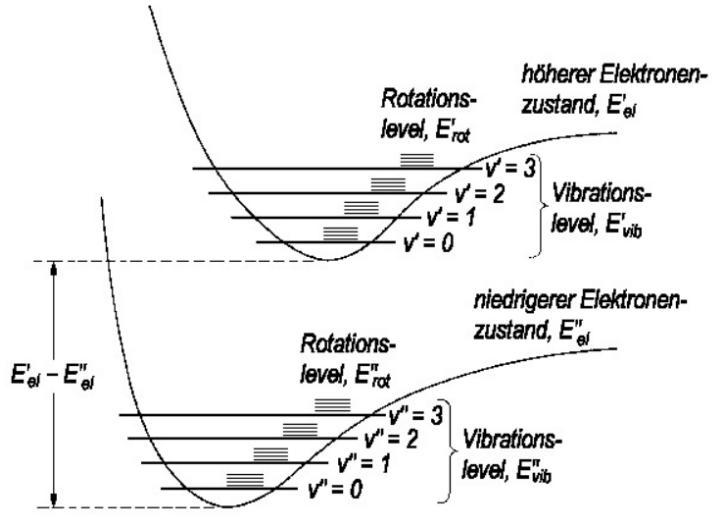

Figure 1: Electronic, vibration and rotation transitions [3].

A transition between the electronic levels gets more probable, if the potentials are over each other. The probability for a transition can be calculated quantum mechanically with the Franck-Condon-factor

$$FC(\nu_i, \nu_k) = \left| \int \Phi_{\text{vib}}(\nu_i) \Phi_{\text{vib}}(\nu_k) \mathrm{d}R \right|^2 \tag{2.3}$$

with the distance R between the two cores and ν_i and ν_j the different energy levels.

2.4. Morse-potential

The Morse-potential describes the electronic potential of a molecule with two atoms, depending on the distance R between the cores. Its can be written as

$$E_{\text{pot}}(R) = D_e \cdot (1 - \exp(-a(R - R_e)))^2 . \tag{2.4}$$

D_e is here the dissociation energy, this is the energy, which the molecule needs in order to break apart, a is a factor. This potential can be seen in Figure 2 in comparison to a parable potential and the real potential of a molecule with two atoms.

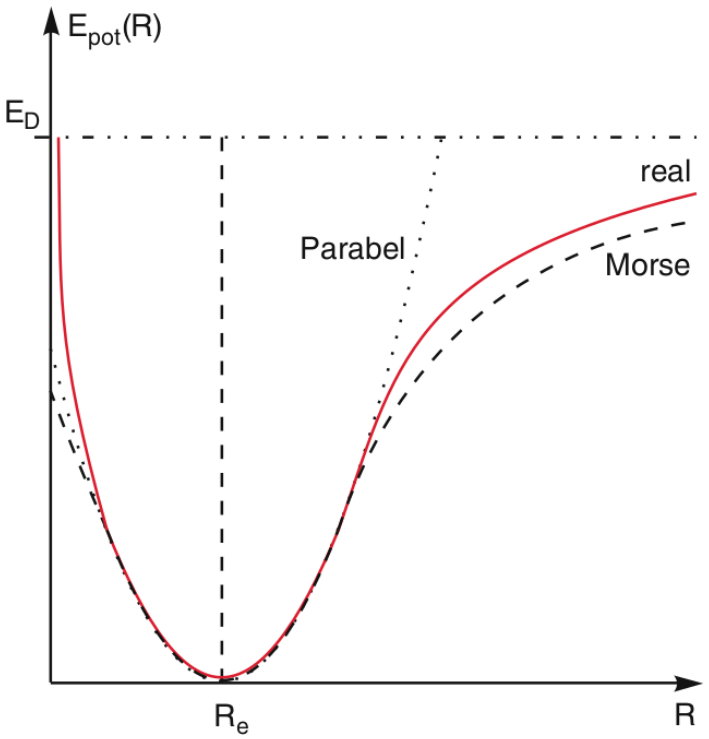

Figure 2: Comparason of a parabel potential, a Morse potential and the real potential of a ground state of a molecule [7, p. 300].

It can be seen, that the Morse potential describes the real potential good in the range between $R = R_e$ and $R \to \infty$. Furthermore it can solve the Schroedinger-equation analytically. The energy eigenvalue is

$$E_{\text{vib}}(\nu) = \hbar\omega_e\left(\nu + \frac{1}{2}\right) - \hbar\omega_e x_e\left(\nu + \frac{1}{2}\right)^2, \tag{2.5}$$

with the vibration constants ω_e and $\omega_e x_e$. By comparing this formula with that shown in [7], it is possible to calculate the dissociation energy

$$D_e = \frac{\omega_e^2}{4\omega_e x_e}. \tag{2.6}$$

2.5. Birge-Sponer plot

One way to calculate the dissociation energy D_e was discovered by Birge and Sponer.
First we need the reduced energy

$$G(\nu) = \frac{E_{\text{vib}}}{\hbar}. \tag{2.7}$$

Now we look at the difference between two neighbour vibration modes. With the Morse potential in mind (Equation 2.5) we get

$$G(\nu+1) - G(\nu) = \omega_e\left(\nu + \frac{3}{2}\right) - \omega_e x_e\left(\nu + \frac{3}{2}\right)^2 - \omega_e\left(\nu + \frac{1}{2}\right) - \omega_e x_e\left(\nu + \frac{1}{2}\right)^2 \tag{2.8}$$

$$= \omega_e - \omega_e x_e\left(1 + 2\left(\nu + \frac{1}{2}\right)\right) := \Delta G(\nu + 1/2). \tag{2.9}$$

If we plot the measured ΔG against $x = \nu + 1/2$ we expect a linear relation. Therefore we can simply do a linear fit with Equation 2.9 as the fit function. We then simply have to plug in the

fit parameters in Equation 2.6.
Birge and Sponer gave us a second way to calculate D_e. First we need to define a reduced energy D_0 as

$$D_0 = \sum_{\nu=0}^{\nu_{\text{diss}}} \Delta G(\nu + 1/2), \tag{2.10}$$

so that we get

$$D_e = G(0) + D_0. \tag{2.11}$$

Since we have a linear relation, the sum in Equation 2.10 can be exchanged with an integral resulting in

$$D_0 = \int_{\nu=0}^{\nu_{\text{diss}}} \Delta G(\nu + 1/2) \tag{2.12}$$

$$= \frac{1}{2}(\omega_e - \omega_e x_e) \cdot \frac{1}{2}\left(\frac{\omega_e}{\omega_e x_e} - 1\right), \tag{2.13}$$

where ν_{diss} is the x-axis intercept in the Birge-Sponer plot. $G(0)$ is calculated with approximating the harmonic oscillator, where the eigenenergies are $E = \hbar\omega(n + 1/2) \Rightarrow \Delta E = 2E(0)$. Therefore we get

$$G(0) = \frac{1}{2}\Delta G(1/2) = \frac{1}{2}(\omega_e - 2\omega_e x_e). \tag{2.14}$$

2.6. Excitation energy T_e and dissociation energy E_{diss}

The energy E_{diss} is the energy needed for the state $\nu'' = 0$ to push the molecule into a higher electron state, where it lies in a region of bound and not bound states. To calculate it we need a progression from $\nu'' = 0$ to a certain ν' with a known wavelength. We then need to add all the $\Delta G's$ for higher progressions.

$$E_{\text{diss}} = G(\nu') + \sum_{\nu'}^{\nu'_{\text{diss}}} \Delta G(\nu' + 1/2). \tag{2.15}$$

For T_e we first need σ_{00}:

$$\sigma_{00} = E_{\text{diss}} - D_0. \tag{2.16}$$

With that we can calculate the excitation energy T_e with

$$T_e = \sigma_{00} - G(0) + \tilde{G}(0), \tag{2.17}$$

where $\tilde{G}(0)$ comes from [2].

3. Setup and procedure

Setup

The setup of this experiment can be seen in Figure 3.

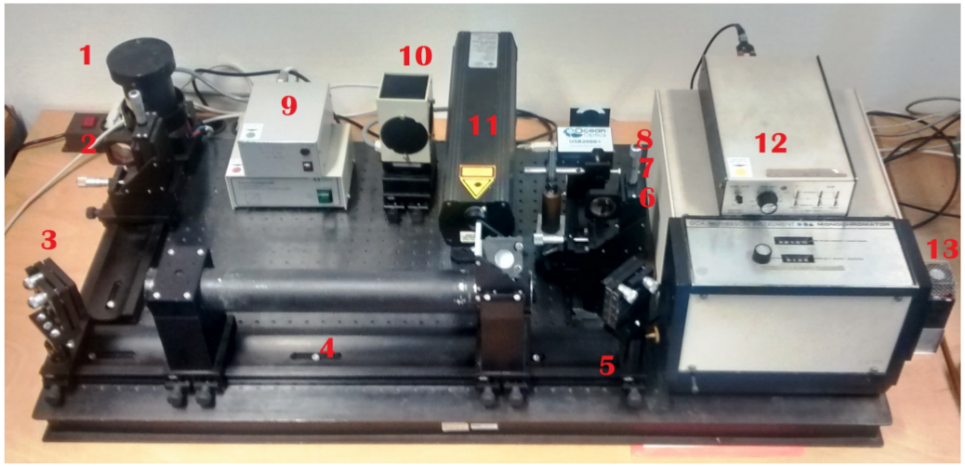

Figure 3: Setup of the experiment from [3].

(1) is a lamp and (3) a mirror, which allows to bring the light into the tube with iodine (4). Behind the tube there is another mirror which is used in the first part of the experiment, where we use a spectrometer (8). We didn't use the lens as shown at (2), but had two lenses at (6), and in the second part at (5). The filter (7) wasn't there, thereby we couldn't use it. For measuring the emission spectrum we didn't use the spectrometer, but a monochromator (12) with a photo multiplier (13). For this experiment a HeNe-laser (11) is needed, which can enter the tube through a mirror. In order to control this setup there is a power supply unit for the peltier cooling of the photo multiplier and that of the photo multiplier. There is also a discriminator. The signals of the spectrometer and the monochromator can be seen and saved on a computer.

Procedure

The first part of the experiment was to measure the absorption spectrum of iodine. For this we used the light of a halogen lamp. This can be used for the absorption, because it has a continuous spectrum. We focused the light on a paper, which we put in front of the spectrometer. When we got it sharp and collimated, we had to change its position a bit, because the opening of the spectrometer isn't directly on the surface of the unit. After we had done this we were able to measure the spectrum with the program SpectraSuite on the computer.
The first task of the second part of the experiment was to calibrate the monochromator. For this we exchanged the halogen lamp with a mercury lamp. From now on we used the monochromator with the photomultiplier. The voltage of the photo multiplier changed while we were measuring between 999 V and 1000 V. We also used the control unit and the discriminator in this part of the experiment. The light of the mercury lamp got focused on the slid of the monochromator. Then we measured the spectrum in a range of 4000 to 6001 Å. After that we turned of the mercury vapour lamp and used a laser instead. Because of the small intensities in the emission spectrum of iodine, we made the room as dark as possible. The difficult part here was to get the laser focused on the slid of the monochromator. Crucial here was to set the lenses in the right order, which wasn't all that easy because they were not marked. Furthermore the slid is again set a bit behind the surface of the device so the light couldn't be focused on the surface. The resonance peak of the laser was measured in a range of 6320 Å and 6352 Å with a step velocity of

2 Å/s. Here the slid had a width of 50 µm. After that we made a measurement between 6400 Å and 8128 Å in order to measure the fluorescence spectrum. Here the step velocity was 1 Å/s and the slid had a width of 370 µm. The software, which was used for measuring everything except for the absorption spectrum, was JodAnalog.

4. Data analysis

The analysis of the data was done using `Python`. For fit functions we used the least-square-fit function `curve_fit` from the `scipy.optimize` package. Some plots won't have errorbars in them. That's due to the fact, that they are either to small to be visible or we omitted them on purpose for the sake of clarity.

4.1. Spectrum of the absorption

In Figure 4 the measured data for the absorption spectrum from a halogen lamp through I_2 is plotted over the wavelength. The data was collected using the given software `SpectraSuit`. We chose an integration time of 0.1 s and set the software to average over 17 measurements. The full header from the data file is shown in the appendix in subsection D.1. The shape of the curve is due to the halogen lamp. The intensity of the continuous spectrum rises from 400 nm to 500 nm slowly, from 500 nm to 620 nm very fast and from 620 nm to 730 nm falls fast down again. We can't say, whether the lamp has also a spectrum below 400 nm or above 730 nm, because the used CCD can't resolve such wavelengths. At 400 nm the intensity suddenly jumps to a higher one. This could be the point, where our CCD starts to measure actual data and before that it is just interference and or noise.
For the y-axis we would have errors following $\sqrt{n}$, but those are to small to be visible in this plot.

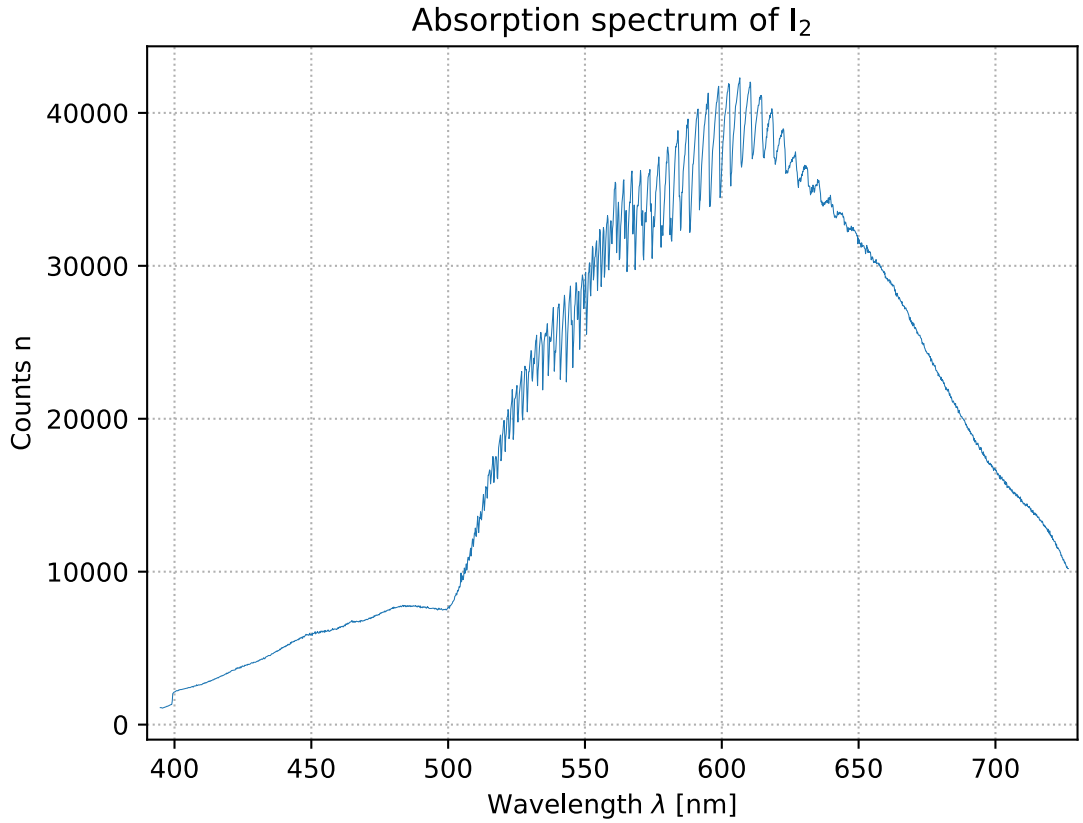

Figure 4: Plotted data for the absorption spectrum.

In Figure 5 a detailed version of the spectra is shown for $500\,\text{nm} < \lambda < 650\,\text{nm}$.

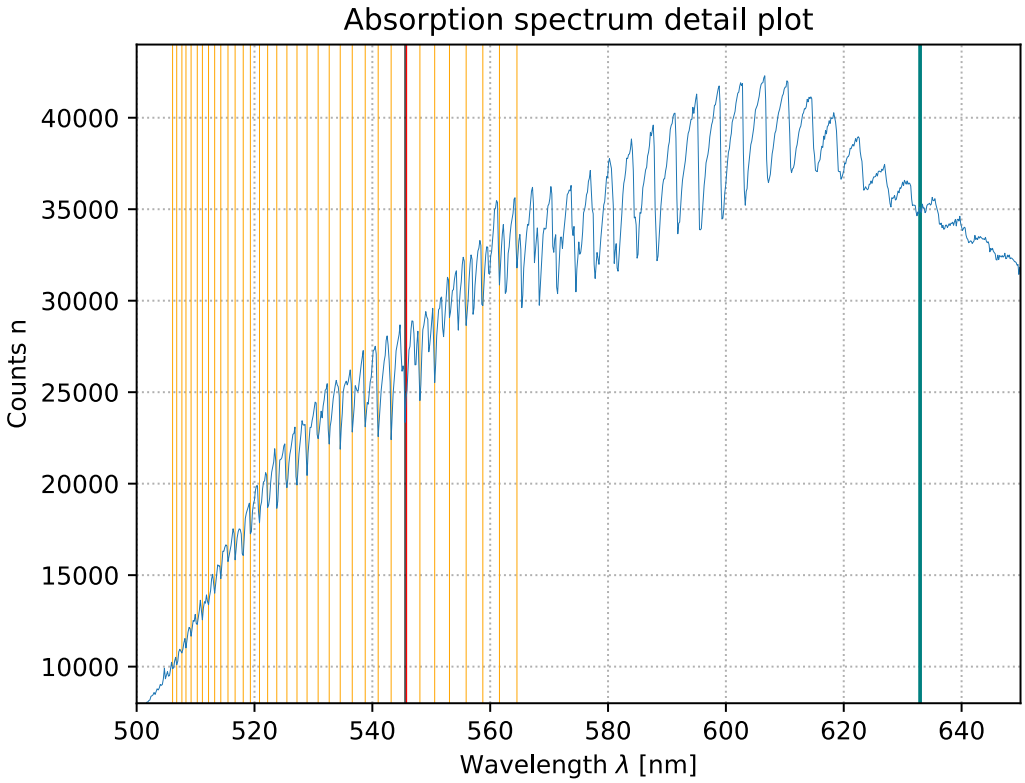

Figure 5: Detail plot for the absorption spectrum.

The teal coloured line at 632.957 nm is the wavelength of our used laser. This is needed later in the emission part. The purple line is the point, where the progression $\nu'' = 0 \rightarrow \nu' = 25$ happens. In the manual it is given that this progression happens at 545.8 nm. In Figure 6 the red line is that given wavelength. We can see, that we didn't measure an absorption at that point, but at 545.55 nm (black line). Therefore we used 545.55 nm for the calculations.

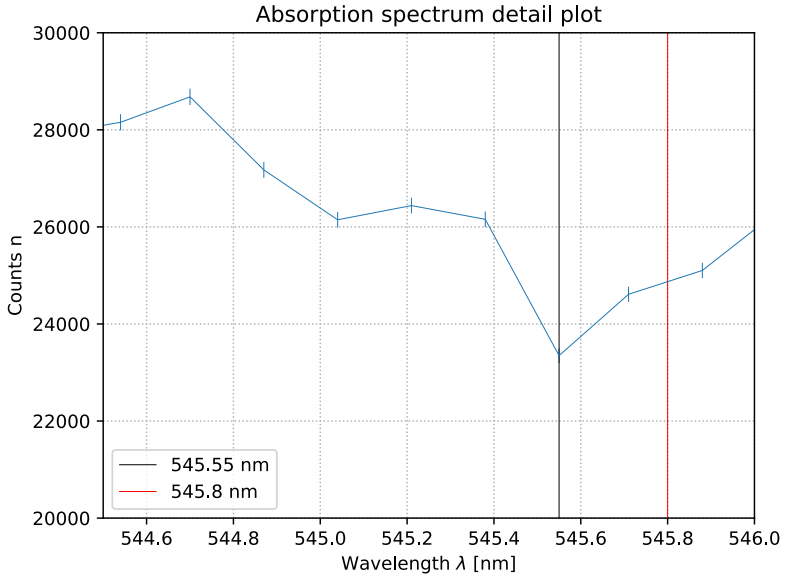

Figure 6: Detailed plot for the progression $\nu'' = 0 \rightarrow \nu' = 25$.

In Figure 5 we draw the lines for all the other progressions belonging to $\nu'' = 0$. Having the Morse potential in mind, the chosen lines are farther apart for lower energies and closer together for higher energies. Therefore the numbers are allocated from right to left, meaning that the lines at the right side have a lower number, than the ones on the left.
For smaller energies/larger wavelengths it gets more and more hard to set lines for the progression having the distance relation in mind. It is most likely that at around 565 nm a different progression starts. As a read off error for the wavelengths we chose 0.0001 nm. The values for our chosen wavelengths are in the appendix in Table 8.

Calculation for the oscillation constants ω_e and $\omega_e x_e$

To make the Birge-Sponer plot, we first need to convert our wavelengths to vacuum wavelengths. To do so, we need to multiply them by the diffraction factor of air

$$\lambda_{\text{vac}} = \lambda_{\text{air}}\ n_{\text{air}}, \tag{4.1}$$

$$s_{\lambda_{\text{vac}}} = \lambda_{\text{vac}} \cdot \frac{s_{\lambda_{\text{air}}}}{\lambda_{\text{air}}}. \tag{4.2}$$

Following [4] we have different factors for different wavelengths. Our data is divided into two groups. The first one needs

$$n_{\text{air}} = 1.000\,279, \tag{4.3}$$

for wavelengths from 500 nm to 540 nm and the second group needs

$$n_{\text{air}} = 1.000\,278, \tag{4.4}$$

for wavelengths from 540 nm to 600 nm.
For the energy G of our photons we need

$$G = \frac{2\pi}{\lambda_{\text{vac}}}, \tag{4.5}$$

with

$$s_G = G \cdot \frac{s_\lambda}{\lambda}. \tag{4.6}$$

Therefore we get

$$\Delta G(\nu + 1/2) = G(\nu+1) - G(\nu) = \frac{2\pi}{\lambda(\nu+1)} - \frac{2\pi}{\lambda(\nu)}, \tag{4.7}$$

with the error

$$s_{\Delta G} = \sqrt{s^2_{G(\nu+1)} + s^2_{G(\nu)}}. \tag{4.8}$$

Having the Morse potential in mind, we expect a linear relation for ΔG and $(\nu + 1/2)$ (see subsection 2.5). Therefore we do a linear fit with

$$\Delta G = \omega_e - \omega_e x_e \cdot (1 + 2(\nu + 1/2)). \tag{4.9}$$

In Figure 7 a reduced ΔG (meaning it is divided by a factor of 2π) is plotted against $(\nu + 1/2)$ to get the oscillation constants directly from the fit function.

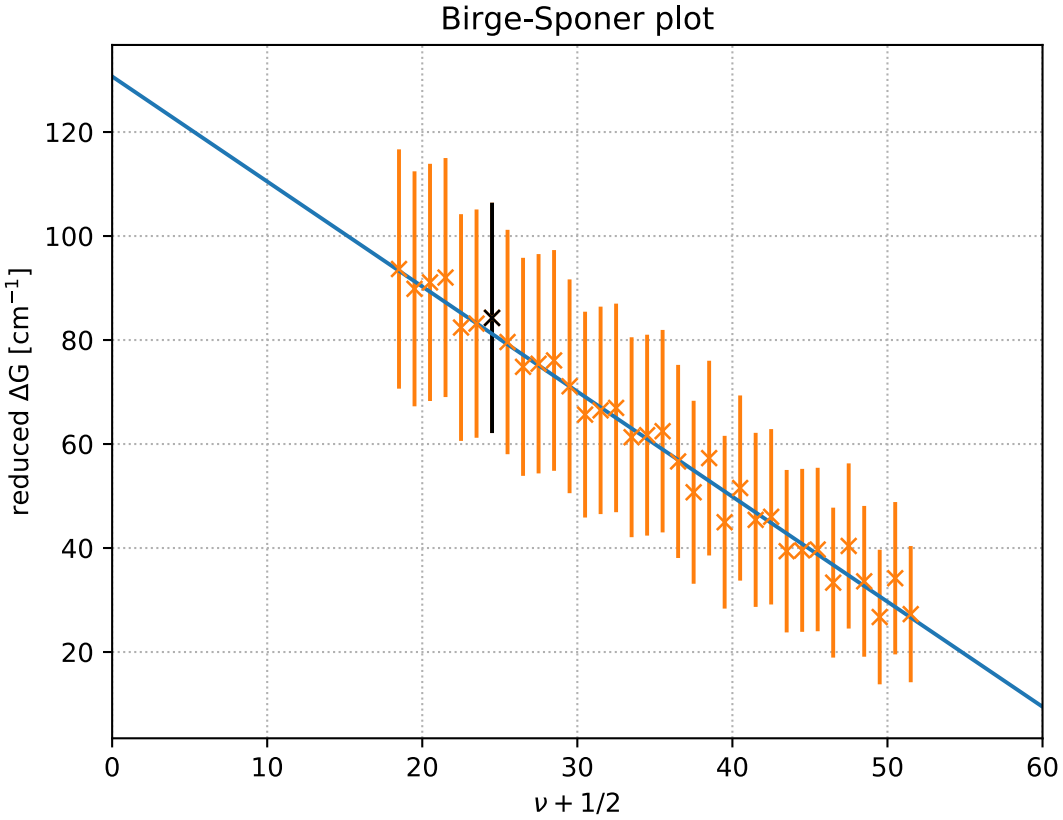

Figure 7: The calculated values for a the Birge-Sponer plot with a linear fit function. The black point is the given progression $\nu'' = 0 \rightarrow \nu' = 25$ but at our measured wavelength of 545.55 nm.

From our fit function we get

$$\omega_e = (131 \pm 2)\,\frac{1}{\text{cm}}, \tag{4.10}$$

$$\omega_e x_e = (1.01 \pm 0.03)\,\frac{1}{\text{cm}}. \tag{4.11}$$

The errors on those values come purely from the covariance matrix of our fit function, therefore we have no statement on the effects from our read off errors on the calculated value. The used `curve_fit` function from the `scipy.optimize` package has an option for an error input, and using this has an effect on the value (only a very small one), but in the package documentation it says, that it is only a least-square fit. Thereby we don't know the effect of giving an error input and didn't use this option.

Calculation of the dissociation energy D_e using the Morse potential and the term difference

With Equation 2.6 and Equation 4.10 we can calculate the dissociation energy D_e with the Morse potential as our underlining theory. We get

$$D_e = (4292 \pm 184)\,\frac{1}{\text{cm}}. \tag{4.12}$$

The error gets propagated from the fit parameter errors with

$$s_{D_e} = D_e \cdot \sqrt{\left(\frac{2s_{\omega_e}}{\omega_e}\right)^2 + \left(\frac{s_{\omega_e x_e}}{\omega_e x_e}\right)^2}. \tag{4.13}$$

The other way to calculate the dissociation energy is described in subsection 2.5. First we need to calculate D_0. With basic Gaussian error propagation we get

$$D_0 = (4227 \pm 184)\,\frac{1}{\text{cm}}. \tag{4.14}$$

Now we need $G(0)$. We calculated

$$G(0) = (65 \pm 3)\,\frac{1}{\text{cm}}. \tag{4.15}$$

Now we can calculate $\tilde{D}_e$ from $D_0 + G(0)$. We get

$$\tilde{D}_e = (4292 \pm 184)\,\frac{1}{\text{cm}}. \tag{4.16}$$

We can see that both values for the dissociation energy are virtually the same. We take the mean value of those and get

$$D_{\text{e, mean}} = (4292 \pm 130)\,\frac{1}{\text{cm}}, \tag{4.17}$$

with basic error propagation.

Calculation of the energy E_{diss}, σ_{00} and the excitation energy T_e

To get the energy, where our molecule dissociates we use

$$E_{\text{diss}} = G(\nu' = 25) + \int_{\nu'=25}^{\nu_{\text{diss}}} \Delta G(\nu + 1/2)\,d\nu \tag{4.18}$$

$$= \frac{1}{\lambda(\nu' = 25)} + \frac{1}{2}(\omega_e - \omega_e x_e(1 + 2 \cdot 25))\left(\frac{1}{2}\left(\frac{\omega_e}{\omega_e x_e} - 1\right) - 25\right) \tag{4.19}$$

$$= (19\,916 \pm 97)\,\frac{1}{\text{cm}}. \tag{4.20}$$

The error is calculated doing Gaussian error propagation. For σ_{00} we get

$$\sigma_{00} = E_{\text{diss}} - D_0 = (15\,689 \pm 208)\,\frac{1}{\text{cm}}. \tag{4.21}$$

For the excitation energy T_e we need $\tilde{G}(0)$ for the groundstate. We get this value from [2], $\tilde{G}(0) = 107\,\text{cm}^{-1}$. With that we can calculate T_e:

$$T_e = \sigma_{00} - G(0) + \tilde{G}(0) = (15\,731 \pm 208)\,\frac{1}{\text{cm}}. \tag{4.22}$$

Plott of the Morse potential with the calculated values

To plot the Morse potential we need $D_{\text{e, mean}}$, a and R_e. R_e and a we can calculate with

$$c = 3 \cdot 10^8\,\frac{\text{m}}{\text{s}}, \qquad \mu = 1.053\,27 \cdot 10^{-25}\,\text{kg} \qquad \text{and} \qquad B_e = (2.897 \pm 0.007)\,\frac{1}{\text{m}}, \tag{4.23}$$

from [5]. We get

$$R_e = \sqrt{\frac{\hbar}{4\pi c \mu B_e}} = (3.028 \pm 0.004)\,\text{Å}, \tag{4.24}$$

and

$$a = \sqrt{\frac{\omega_e x_e 4\pi c \mu}{\hbar}} = (1.95 \pm 0.05)\,\frac{1}{\text{Å}}. \tag{4.25}$$

In Figure 8 we plotted the Morse potential with the calculated and measured values.

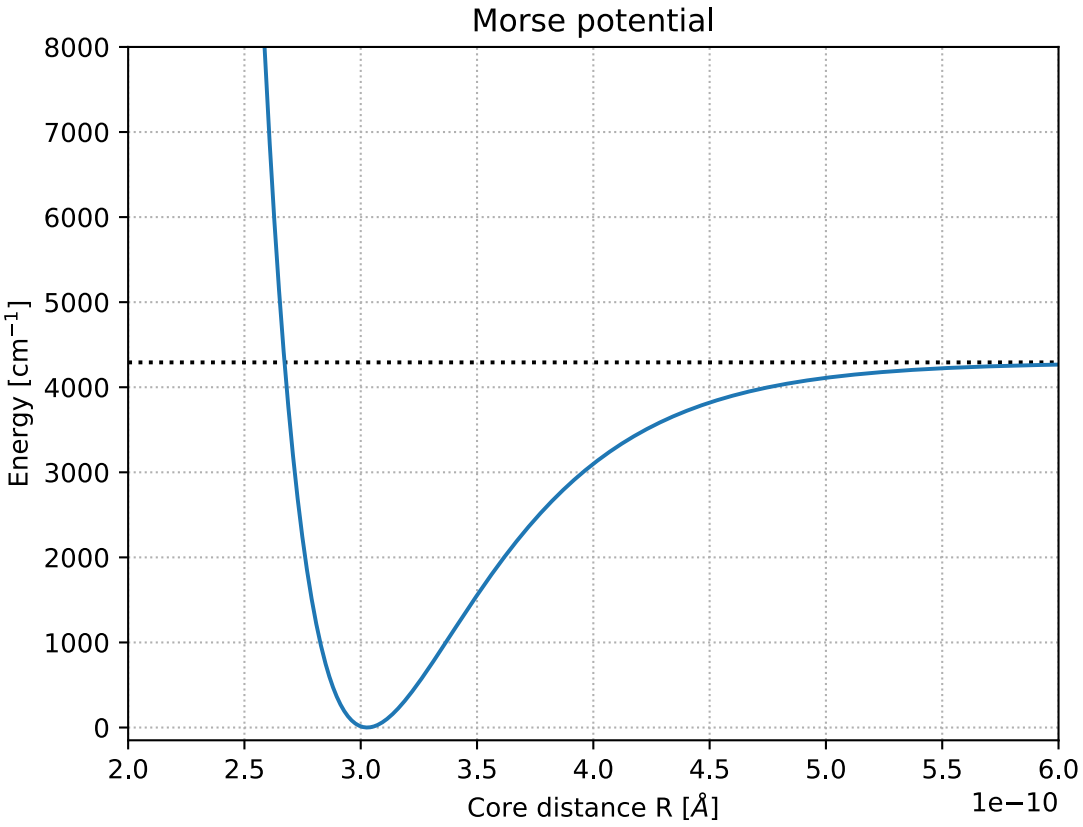

Figure 8: Calculated Morse potential. The black line is $D_{\text{e, mean}}$.

4.2. Spectrum of the emission

In the second part of the experiment we look at the spectrum of the emission of iodine. In order to measure this, the monochromator has to be calibrated. For this we used the spectrum of a mercury vapour lamp. The expected values for lines from [3] are listed in Table 1.

λ [nm]	404.66	435.83	546.07	576.96	579.07
name	h-line	g-line	e-line	orange double rule	

Table 1: Spectral line of a Hg-lamp.

We compare those values we measured for the orange double rule with their corresponding values from literature. We chose these lines for calibration, because the wave lengths of the emission spectrum of I_2 will be bigger, so that these are the closest lines we have for comparison. Our original data had an offset of 2.63 Å, so we shifted it for this value. The result can be seen in Figure 9.

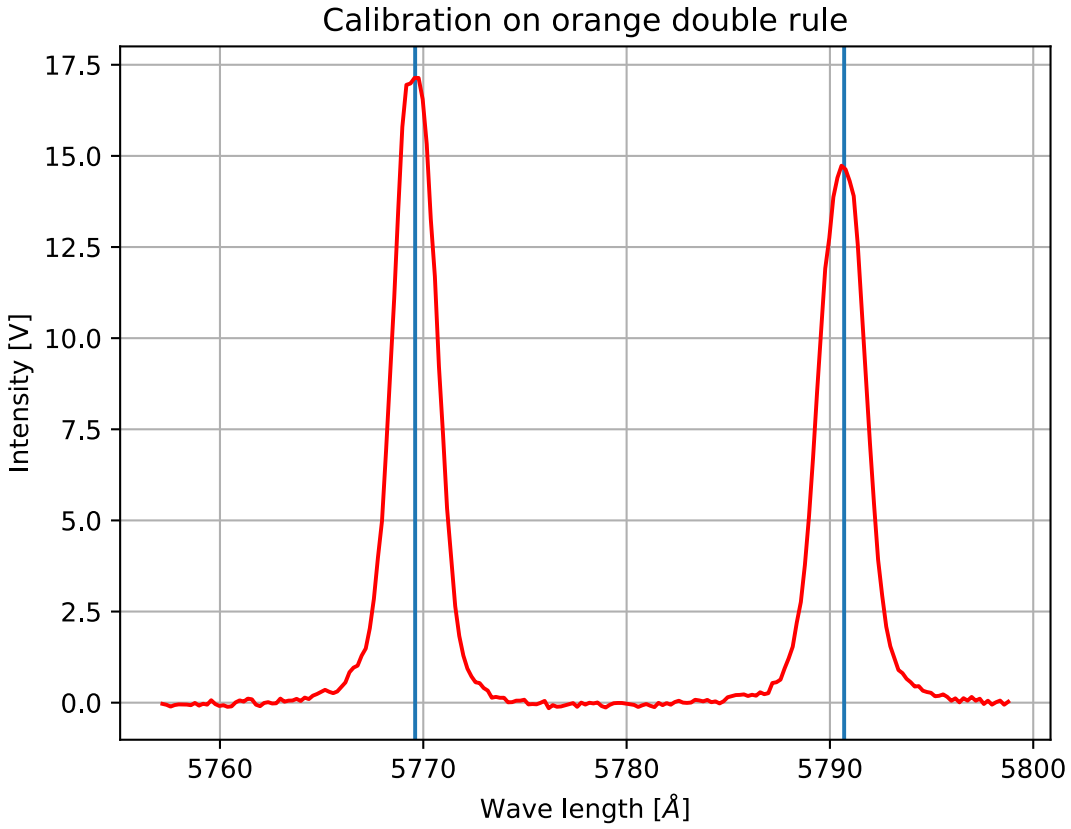

Figure 9: Calibration with orange double rule.

Because of the broadness of the peaks and by comparing them to Figure 10 and Figure 13, 14 and 15 in the appendix, we chose an error of $s_\lambda = 5$ Å on the wavelength. Since the effect of the diffraction factor is smaller than the error, we neglected it. The fact, that none of the spectral lines is flat on top, indicates, that the discriminator was set correctly and didn't overmodulate.

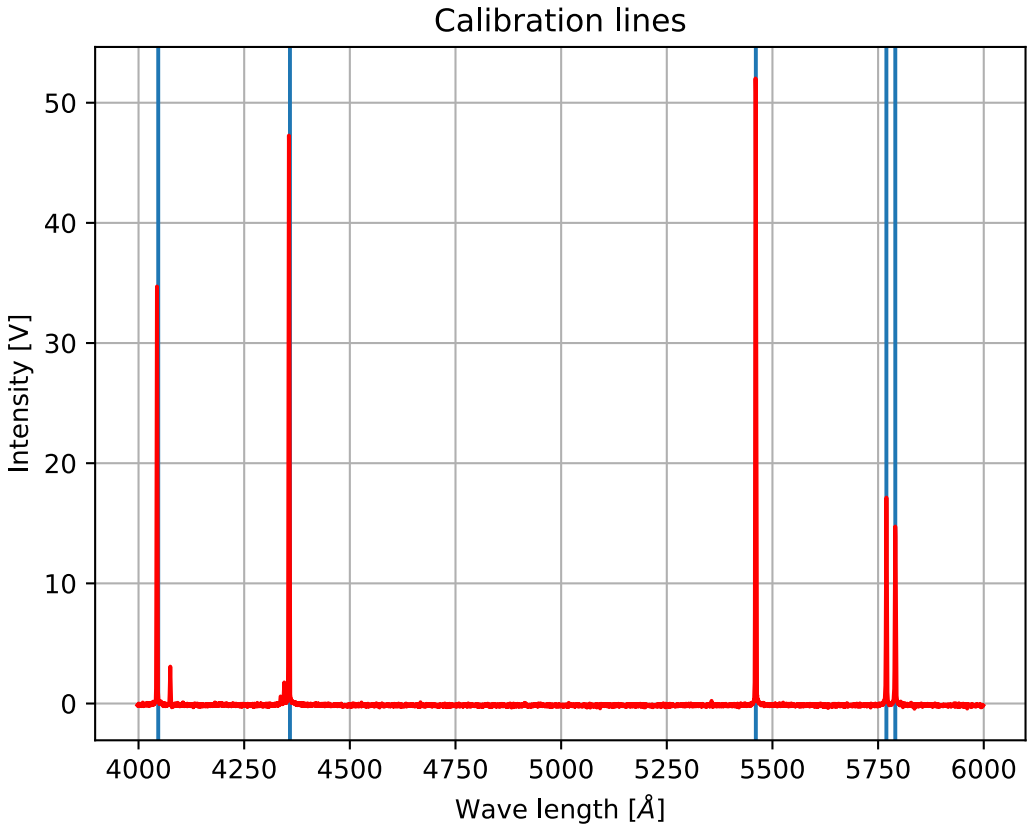

Figure 10: Total spectrum of the calibration.

Especially the plots in Figure 13 and Figure 14 show some differences between our maximum and that from literature. This indicates, that there might be some problems in comparing wave length, that are far away from the orange double rule, to those from literature.

After finishing the calibration, we can start analysing the measured data of the emission spectrum of I_2. Because of very different intensities, the spectrum gets measured in two parts. At first the width of the aperture is much smaller ($d = 50\,\mu m$) and we measured in a range of $\lambda =$ 6320 Å to 6350 Å. The plot can be seen in Figure 11.

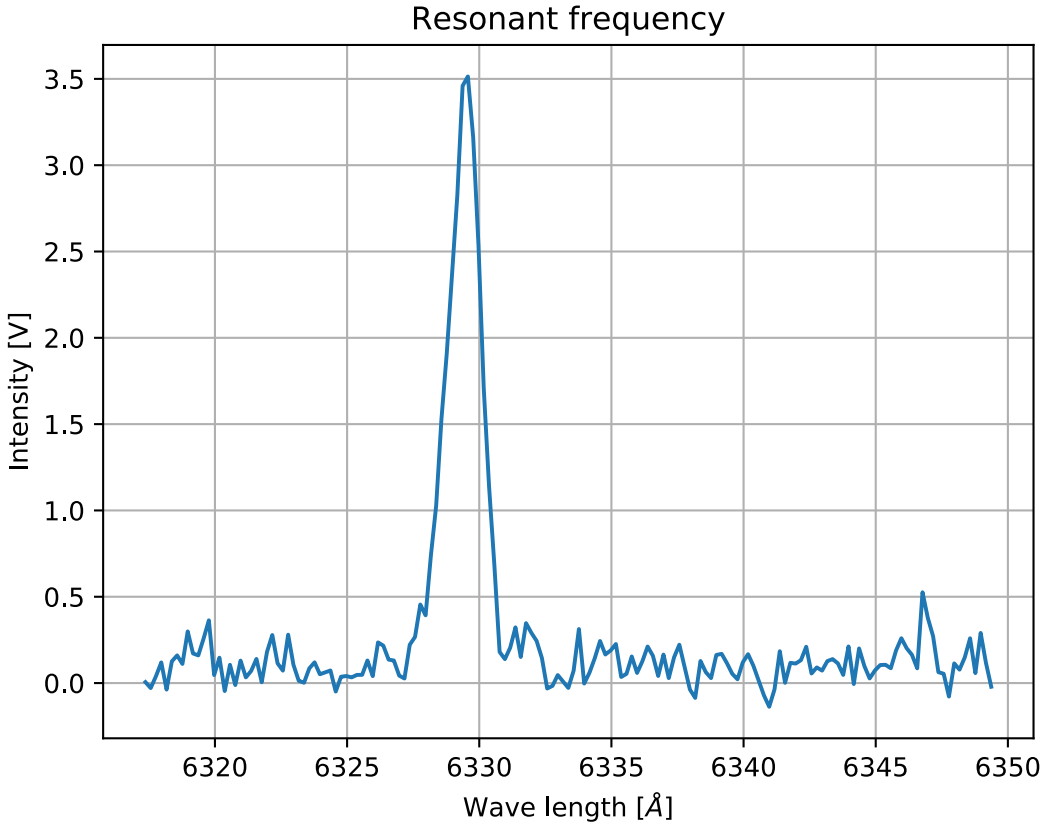

Figure 11: Resonant frequency of the laser.

For the position of the maximum we get a wave length of

$$\lambda = (6329 \pm 5)\,\text{Å}. \tag{4.26}$$

The error on a Gaussian fit can be neglected compared to the error we got by the calibration. By taking again a look at Figure 6, we see, that the teal coloured line fits a dip in that spectrum very nicely. This makes sense, because the same energy is needed in order to get a maximum in the emission spectrum as to get a minimum in the emission spectrum.
In the second measurement the aperture gets widened to $d = 370\,\mu\text{m}$. The reason for this is, that the intensities of the fluorescence spectrum are much smaller. This makes this measurement much more difficult, than the ones before, because it is very hard to remove most of the noise but see as many peaks as possible. The data we got is plotted in Figure 12.

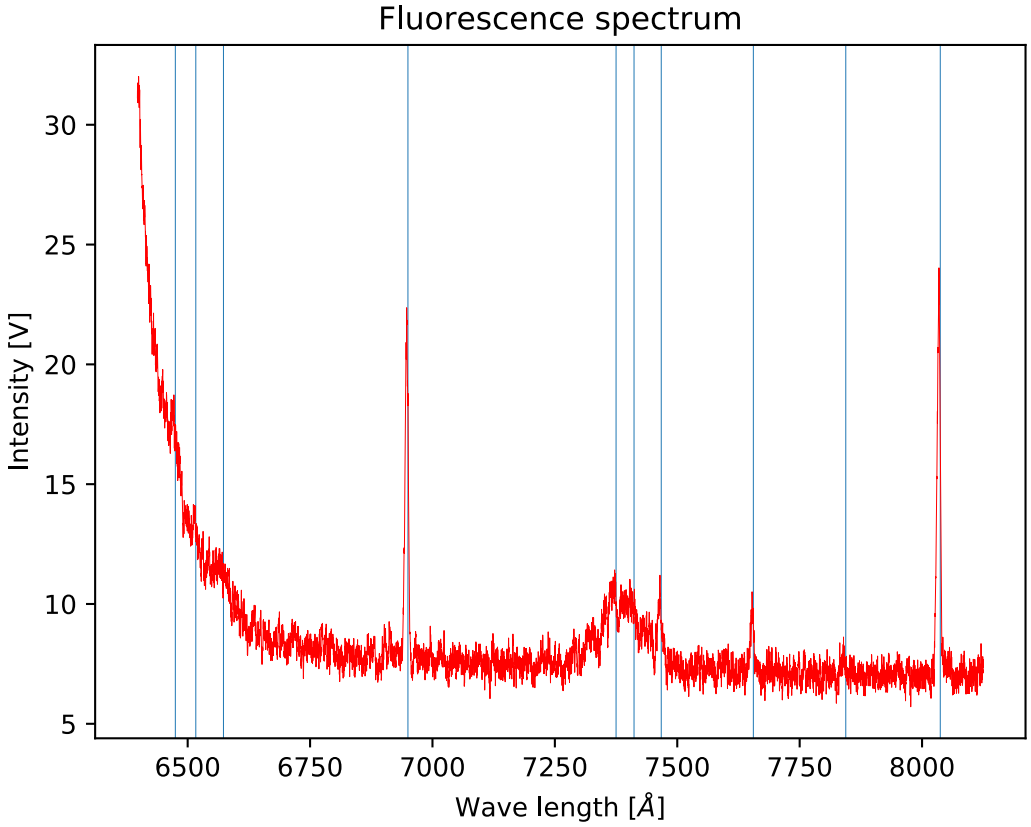

Figure 12: Measured emission spectrum.

The vertical lines indicate the maxima we assumed to be spectral lines. There are some other wave length, that could be read as spectral lines, but because of the noise we couldn't be sure. Those wave lengths shown in the plot are listed in Table 2. The errors here are read off errors.

	Wavelength [Å]
λ_1	6474 ± 10
λ_2	6516 ± 10
λ_3	6573 ± 10
λ_4	6949 ± 10
λ_5	7375 ± 10
λ_6	7411 ± 10
λ_7	7467 ± 10
λ_8	7655 ± 10
λ_9	7844 ± 10
λ_{10}	8037 ± 10

Table 2: Spectral lines of I_2.

This data can be compared to Figure 5. The peaks of the absorption end there around 6500 Å. Here the first detected peak is at (6474.8 ± 0.5) Å. In order to identify the transitions of a progression $\nu' \to \nu''$ we have to search for equidistant peaks. The transitions, that we were able to identify for the progression $\nu' = 1 \to \nu''$ are listed in Table 3 and for the progression $\nu' = 2 \to \nu''$ in Table 4.

	k [cm^{-1}]	ν''	k_{lit} [cm^{-1}]
λ_1	$15\,444 \pm 24$	1	15 424.5088
λ_3	$15\,213 \pm 24$	3	15 213.6508
λ_4	$14\,388 \pm 20$	7	14 382.3588
λ_5	$13\,559 \pm 18$	11	13 570.4908
λ_7	$13\,391 \pm 18$	12	13 370.5588

Table 3: Identification of the transitions in the progression $\nu' = 1 \to \nu''$, with literature values from [4].

	k [cm^{-1}]	ν''	k_{lit} [cm^{-1}]
λ_6	$13\,492 \pm 18$	12	13 493.0588
λ_8	$13\,062 \pm 18$	14	13 096.8368
λ_9	$12\,748 \pm 16$	16	12 705.4708

Table 4: Identification of the transitions in the progression $\nu' = 2 \to \nu''$, with literature values from [4].

We also found one peak of the progression $\nu' = 4 \to \nu''$ and one for $\nu' = 3 \to \nu''$. Both are listed in Table 5.

	k [cm^{-1}]	ν''	k_{lit} [cm^{-1}]
λ_2	$15\,346 \pm 24$	4	15 367.3068
λ_{10}	$12\,442 \pm 16$	19	12 440.0608

Table 5: Identification of the transitions in the progression $\nu' = 3 \to \nu''$, with literature values from [4].

From the wavelengths we calculate the wave numbers k and compare this to values from [4]. The uncertainty of the inverse wave length is calculated with

$$s_k = k\frac{s_\lambda}{\lambda}. \tag{4.27}$$

The fact, that there are always some gaps between the progressions, indicates, that we lost some emission lines in the noise. With our data it isn't possible to say which progression is the one belonging to the laser.
In order to calculate the height of the peaks, one can use the Franck-Condon-factors. Their calculation is described in [4]. In the following we will summarise the way how to calculate them. The formulas, that are needed are

$$FC(\nu_i, \nu_k) = \left| \int \Psi_{\text{vib}}(\nu_i)\Psi_{\text{vib}}(\nu_k)\mathrm{d}R \right|^2 \tag{4.28}$$

$$\Psi_{\text{vib}}(\nu) = N_\nu H_\nu(x) e^{-R^2/2} \tag{4.29}$$

$$N_\nu = \frac{1}{\sqrt{2^\nu \nu! \pi}} \tag{4.30}$$

$$H_\nu = (-1)^\nu e^{x^2} \frac{d^\nu}{dx^\nu} e^{-x^2} \tag{4.31}$$

$$x = \frac{R - R_0}{\sqrt{\frac{\hbar}{\sqrt{\mu k}}}}. \tag{4.32}$$

ν is the vibration quantum number, the distance between the cores is given here as R, R_0 is the equilibrium distance between the potentials of each state which is known for the excited state and mustn't be looked at for the ground state. μ is the known reduced mass of I_2 and k is the force constant of a harmonic oscillator. It can be calculated with the second derivation of the Morse potential. From this follows, that k depends on E_D, a and R_e which are all known. With these data it is possible to calculate for known ν_i and ν_k the Franck-Condon-factors. While comparing these factors with the height of the peaks, it is necessary to remember, that the first two peaks are on an exponential underground.

5. Summary and discussion

The first part of the experiment was about the absorption spectrum. We could calculate the following values with their literature value counterpart from [6]:

		measured value	literature value
ω_e	$[\mathrm{cm}^{-1}]$	131 ± 2	125
$\omega_e x_e$	$[\mathrm{cm}^{-1}]$	1.01 ± 0.03	0.70
D_e	$[\mathrm{cm}^{-1}]$	4292 ± 130	4391
E_{diss}	$[\mathrm{cm}^{-1}]$	$19\,916 \pm 97$	-
T_e	$[\mathrm{cm}^{-1}]$	$15\,731 \pm 208$	15 711
a	$[\text{Å}^{-1}]$	1.95 ± 0.05	-
R_e	[Å]	3.028 ± 0.004	3.028

We see that ω_e is in a 3σ range to the literature value, with a relative error of 1.5 %, therefore being a reasonable result. $\omega_e x_e$ is in a 11σ range with a relative error of 2.9 %. With such a small relative error we would conclude, that there must be a systematic offset. The measured spectrum from our CCD could have a shift on the x-axis. That would change the wavelengths, but the difference between two neighbour wavelengths/energies wouldn't change. A y-axis offset in our CCD wouldn't affect our wavelengths at all. Therefore our CCD can't be the origin of an offset for ω_e and $\omega_e x_e$.
Since the errors on those two values come purely from our fit function and are not propagated from our read off errors for the wavelengths, we need to take a closer look at those errors. In Figure 7 we can see, that the read off errors are enormous in comparison to our y-axis error from our fit function. If we took those errors into account, our errors for ω_e and $\omega_e x_e$ would be much bigger and therefore pushing us into a smaller σ range to the literature value. Obviously the relative error would rise for those values as well, but we could improve our read off errors, by choosing a more precise read off method, for example fitting inverted Gaussians onto the troughs in Figure 5 and or using a CCD with a higher x-axis resolution to get more data points around the troughs. With that we then could make an assumption, whether there is a systematic error/offset caused by our measure method or not.
D_e got calculated in two different ways. The first one was to have the Morse potential as the underlining theory and calculate it with Equation 2.6. The other way was to calculate it through a term difference. Both gave us the same result and the same error. Therefore we took the median and propagated their error. D_e, T_e and R_e are all in a one σ interval with their corresponding literature value. This is surprising, since they are calculated, using ω_e and $\omega_e x_e$ which are quite off of the real value. D_e has a relative error of 3 %, T_e 1.3 % and R_e 0.13 %. For E_{diss} we don't have a literature value, but since it is used to calculate T_e, which is very close to the literature value and very precise, we conclude, that it should be also very close to the real value and is very precise, since it has a relative error of 0.5 %. For a we also have no literature value. It has a relative error of 1.7 %. For all those values we have to keep in mind, that their error is propagated from the fit function errors and not from the read off errors for the wavelengths.

The second part of the experiment was about the emission spectrum. With a mercury vapour lamp it was possible to adjust the data gained from a monochromator. With these corrections we got

$$(6329 \pm 5)\,\text{Å}$$

as the wavelength of the laser, which is in a 1σ range of the literature value from [3]. This value is 6330 Å. This indicates, that the calibration was done well. A major problem occurred

in the measurement of the fluorescence spectrum. Here it wasn't possible to get noise further down with the discriminator, without loosing the peaks. This made it impossible to see small resonance maxima. Following from this we only were able to identify ten maxima. In the room in which the experiment took place there are quiet some sources for the noise, for example control lamps and screens of computers. Furthermore while we were measuring in the same room, there was another group, which used flashlights in order to see something on their setting. The light in the room could be reduced by measuring the background. For this it would be essential, that the wave lengths fit perfectly to those of the measurement. Another possible source of the noise is, that there was to few gaseous iodine in the tube. Following from that the smaller peaks couldn't emit enough light to be seen through the noise and the not gaseous iodine absorbs some of the light.
We assume, that the most important error in this experiment is that on the wavelength. This is due to the fact, that the calibration of the data was done with just two wave lengths, which were quiet close. This gave a rather good calibration for some lines (e-line of the mercury, resonance frequency of the laser), but at some other lines differences can be seen (g-line, h-line). Another possible source of errors on the wavelength is, that the motor, that moves the grid in the monochromator, might not always have the same velocity. This can't be checked, because we only can average over the total time of measurement. Furthermore we can't know how good the lattice is, that is installed in the monochromator. All of these errors could have been reduced, if the wavelength, which is detected by the monochromator, and that which is the x-axis of our data on the computer would be synchronised automatically.
In the emission spectrum of iodine we found ten intensity maxima. We were able to identify most transitions as belonging to two progressions: $\nu' = 1 \to \nu''$ and $\nu' = 3 \to \nu''$. The results are listed in Table 6 and Table 7 together with the difference between the measured data and the values from the literature.

	k [cm^{-1}]	ν''	k_{lit} [cm^{-1}]	σ
$\lambda_1 = (6474 \pm 5)$ Å	$15\,444 \pm 24$	1	15 424.5088	1
$\lambda_3 = (6573 \pm 5)$ Å	$15\,213 \pm 24$	3	15 213.6508	1
$\lambda_4 = (6949 \pm 5)$ Å	$14\,388 \pm 20$	7	14 382.3588	1
$\lambda_5 = (7375 \pm 5)$ Å	$13\,559 \pm 18$	11	13 570.4908	1
$\lambda_7 = (7467 \pm 5)$ Å	$13\,391 \pm 18$	12	13 370.5588	2

Table 6: Transitions in the progression $\nu' = 1 \to \nu''$, with literature values from [4].

	k [cm^{-1}]	ν''	k_{lit} [cm^{-1}]	σ
$\lambda_6 = (7411 \pm 5)$ Å	$13\,492 \pm 18$	12	13 493.0588	1
$\lambda_8 = (7655 \pm 5)$ Å	$13\,062 \pm 18$	14	13 096.8368	2
$\lambda_9 = (7844 \pm 5)$ Å	$12\,748 \pm 16$	16	12 705.4708	3

Table 7: Transitions in the progression $\nu' = 2 \to \nu''$, with literature values from [4].

We assume, that the last peak (at $\lambda_{10} = (8037 \pm 5)$ Å) belongs to the progression $\nu' = 3 \to \nu''$, because here the literature value and our measured value are in a 1σ range. The peak at $\lambda_2 = (6516 \pm 5)$ Å might belong to the progression $\nu' = 4 \to \nu''$ with a 2σ range, but since it is only a very small peak, we can't exclude, that this is simply some noise. Since none of the k's has a relative error bigger than $s_{rel} = 1\,\%$, and most data is in small σ-ranges to the literature, we can say, that our measurement gave quite good results. We assume, that the reason, why there are gaps between the ν'' in our lists, results in the noise and the fact, that those peaks are probably very small. These small differences between the theoretical values and our data shows our trouble in choosing which progression from the level the iodine had been excited to.

Another possible reason for this difficulty is, that there was some error in iodine tube. This we couldn't check, because the tube was closed, but was discovered by a different group after us. We weren't able to calculate the heights of the peaks with the Franck-Conan-factors, but we described the way, with which it could be done.

A. List of Figures

B. List of Tables

C. References

[1] D. Meschede ed.: *Gerthsen Physik*, Springer-Verlag Berlin Heidelberg, 2015

[2] K.P. Huber and G. Herzberg, U.S. Secretary of Commerce on behalf of the U.S.A., `https://webbook.nist.gov/cgi/inchi/InChI%3D1S/I2/c1-2`

[3] M. Meyer: *Versuchsanleitung Fortgeschrittenen Praktikum Spektroskopie am Jod-Molekül* Physikalisches Institut, Fakultät für Mathematik und Physik, Albert-Ludwigs-Universität Freiburg, 2014

[4] M.Meyer: *Verbesserung des Versuchs Spektroskopie am J_2-Molekül des Fortgeschrittenen Praktikums*, Wissenschaftliche Arbeit für das Staatsexamen im Fach Physik, Physikalisches Institut Albert-Ludwig-Universität Freiburg, 2014

[5] K. BITSCH: *Aufbau einer Apparatur fürs Fortgeschrittenen-Praktikum: „ Untersuchung der Schwingungsstruktur des $B^3\Pi^+_{0g} \rightarrow X^1\Sigma^+_{0g}$ - Übergangs beim I_2 -Molekül "*, Freiburg i. Br. 1977

[6] J. I. Steinfeld, R. N. Zare, L. Jones, M. Lesk, W. Klemperer: *Spectroscopic Constants and Vibrational Assignment for the $B^3\Pi_{0u}^+$ State of Iodine*, Journal of Chemical Physics, Volume 42, Number 1; 1. Januar 1965

[7] W. Demtröder: *Experimentalphysik 3 - Atome, Moleküle und Festkörper*, Springer-Verlag Berlin Heidelberg 2016

D. Appendix

D.1. Absorption

ν'	52	51	50	49	48	47	46	45	44
λ [nm]	506.1	506.8	507.68	508.37	509.24	510.29	511.16	512.2	513.24
ν'	43	42	41	40	39	38	37	36	35
λ [nm]	514.28	515.5	516.71	518.09	519.3	520.85	522.23	523.78	525.5
ν'	34	33	32	31	30	29	28	27	26
λ [nm]	527.21	528.92	530.8	532.68	534.55	536.59	538.79	540.99	543.19
ν'	25	24	23	22	21	20	19	18	
λ [nm]	545.55	548.07	550.58	553.09	555.92	558.75	561.57	564.5	

Table 8: Wavelengths of the progressions.

Header from the data file from `SpectraSuite`

```
SpectraSuite Datei
++++++++++++++++++++++++++++++++++
Datum: Thu Jan 01 05:34:06 CET 2004
Benutzer: Student
Dark-Spektrum vorhanden: Nein
Referenz-Spektrum vorhanden: Nein
Zahl der probierten Teilspektren: 1
Spektrometer: USB2+H15728
Integrationszeit (usec): 100000 (USB2+H15728)
Spektren Durchschnitt berechnet: 17 (USB2+H15728)
Boxcar Glättung: 0 (USB2+H15728)
Dunkelstromkorrektur: Nein (USB2+H15728)
Puls/Lampe aktiviert: Nein (USB2+H15728)
Correct for Detector Non-linearity: Nein (USB2+H15728)
Streulichtkorrektur: Nein (USB2+H15728)
Anzahl Pixel in verarbeitetem Spektrum: 2048
>>>>>Begin Processed Spectral Data<<<<<
394,80 1110,52
394,99 1110,52
395,18 1110,52
[...]
726,41 10203,50
726,54 10203,50
726,67 10203,50
>>>>>End Processed Spectral Data<<<<<
```

D.2. Additional plots for the emission

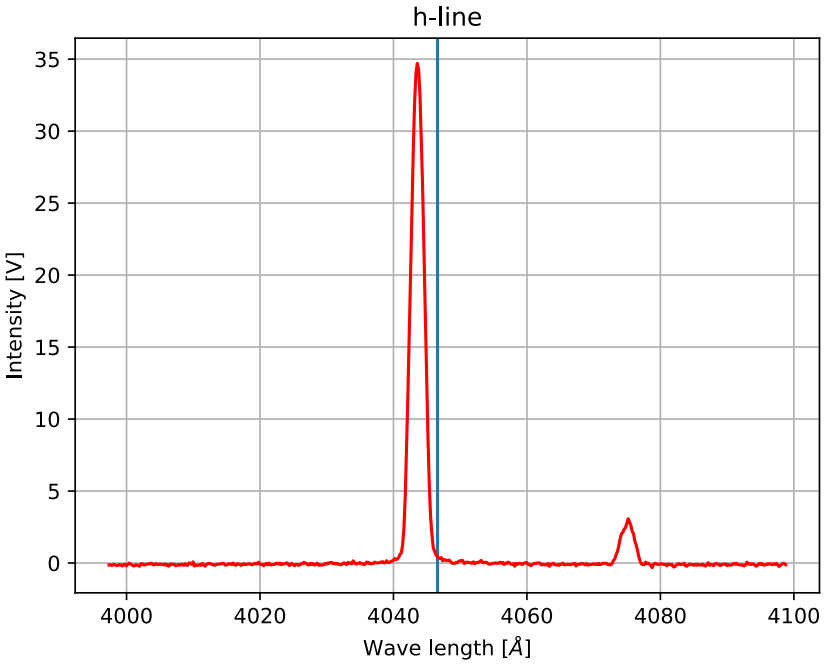

Figure 13: Data and literature value for the h-line.

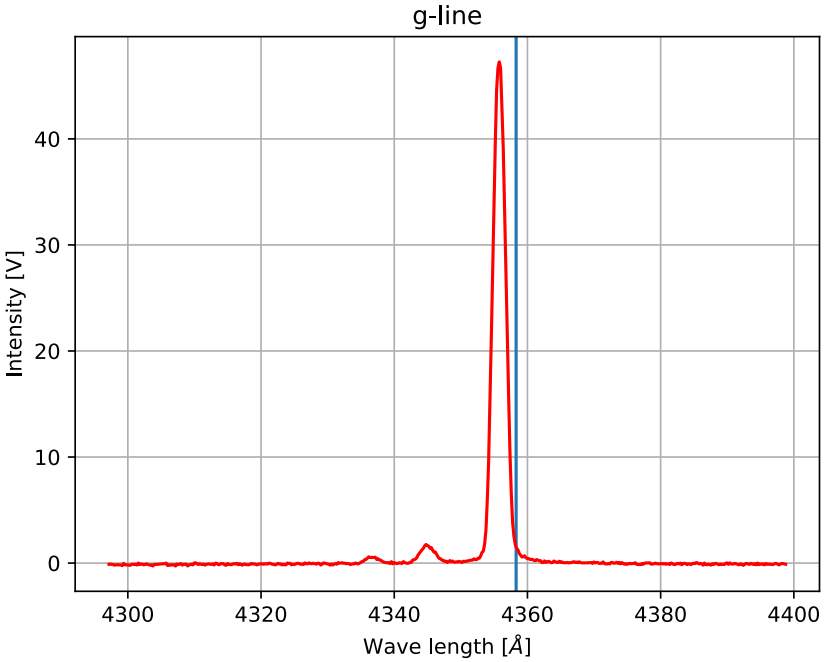

Figure 14: Data and literature value for the g-line.

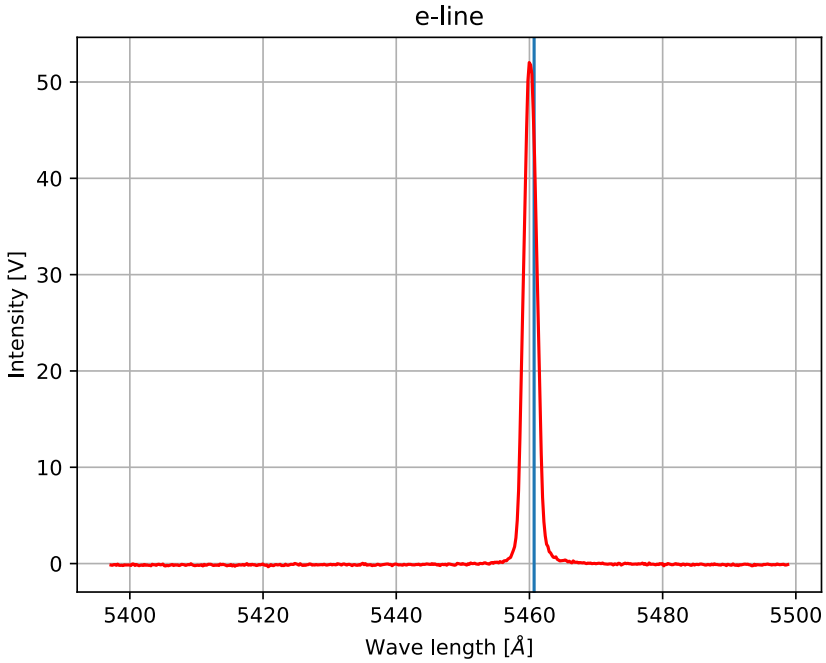

Figure 15: Data and literature value for the e-line.

D.3. Table for determination of transitions

v'	G'(v')	v''	G''(v'')	k(v'=1)	k(v'=2)	k(v'=3)	k(v'=4)	k(v'=5)	k(v'=6)
1	186,375	1	320,38425	15636,5808	15759,0808	15880,1808	15999,8808	16118,1808	16235,0808
2	308,875	2	532,45625	15424,5088	15547,0088	15668,1088	15787,8088	15906,1088	16023,0088
3	429,975	3	743,31425	15213,6508	15336,1508	15457,2508	15576,9508	15695,2508	15812,1508
4	549,675	4	952,95825	15004,0068	15126,5068	15247,6068	15367,3068	15485,6068	15602,5068
5	667,975	5	1161,38825	14795,5768	14918,0768	15039,1768	15158,8768	15277,1768	15394,0768
6	784,875	6	1368,60425	14588,3608	14710,8608	14831,9608	14951,6608	15069,9608	15186,8608
		7	1574,60625	14382,3588	14504,8588	14625,9588	14745,6588	14863,9588	14980,8588
		8	1779,39425	14177,5708	14300,0708	14421,1708	14540,8708	14659,1708	14776,0708
		9	1982,96825	13973,9968	14096,4968	14217,5968	14337,2968	14455,5968	14572,4968
		10	2185,32825	13771,6368	13894,1368	14015,2368	14134,9368	14253,2368	14370,1368
		11	2386,47425	13570,4908	13692,9908	13814,0908	13933,7908	14052,0908	14168,9908
		12	2586,40625	13370,5588	13493,0588	13614,1588	13733,8588	13852,1588	13969,0588
		13	2785,12425	13171,8408	13294,3408	13415,4408	13535,1408	13653,4408	13770,3408
		14	2982,62825	12974,3368	13096,8368	13217,9368	13337,6368	13455,9368	13572,8368
		15	3178,91825	12778,0468	12900,5468	13021,6468	13141,3468	13259,6468	13376,5468
		16	3373,99425	12582,9708	12705,4708	12826,5708	12946,2708	13064,5708	13181,4708
		17	3567,85625	12389,1088	12511,6088	12632,7088	12752,4088	12870,7088	12987,6088
		18	3760,50425	12196,4608	12318,9608	12440,0608	12559,7608	12678,0608	12794,9608
		19	3951,93825	12005,0268	12127,5268	12248,6268	12368,3268	12486,6268	12603,5268
		20	4142,15825	11814,8068	11937,3068	12058,4068	12178,1068	12296,4068	12413,3068
		21	4331,16425	11625,8008	11748,3008	11869,4008	11989,1008	12107,4008	12224,3008
		22	4518,95625	11438,0088	11560,5088	11681,6088	11801,3088	11919,6088	12036,5088
		23	4705,53425	11251,4308	11373,9308	11495,0308	11614,7308	11733,0308	11849,9308
		24	4890,89825	11066,0668	11188,5668	11309,6668	11429,3668	11547,6668	11664,5668
		25	5075,04825	10881,9168	11004,4168	11125,5168	11245,2168	11363,5168	11480,4168
		26	5257,98425	10698,9808	10821,4808	10942,5808	11062,2808	11180,5808	11297,4808
		27	5439,70625	10517,2588	10639,7588	10760,8588	10880,5588	10998,8588	11115,7588
		28	5620,21425	10336,7508	10459,2508	10580,3508	10700,0508	10818,3508	10935,2508
		29	5799,50825	10157,4568	10279,9568	10401,0568	10520,7568	10639,0568	10755,9568
		30	5977,58825	9979,37675	10101,8768	10222,9768	10342,6768	10460,9768	10577,8768

Figure 16: Data for the determination of transitions in the emission spectrum from [4].

D.4. Original data

I2 - Molekül 21.09.18

~~Kalibrierung~~ Absorption: Datei test2.txt

Emission Absorption Temp.: 27,2°C

Spannung: schwankt 999 - 1000 V

Diskriminator: Time const. 1 s

I) ~~Kali~~ Kalibration: Step 2 Å/s

Beginn 4000 Å

Ende: 6001 Å

Datei: Kalibrierung-1.dat

II) Laser Peak:

Scan Rate: 2 Å/s

Beginn: 6320 Å

Ende: 6352 Å

Slid: 50 µm

Datei: Laserpeak-2Step.dat

III) Spektrum

Scan Rate: 1 Å/s

Beginn 6400 Å

Ende: 8127 Å

Slid width: 370 µm

Datei: Laser-1Step-5.dat